

since these cell types provide high conversion rates even at high flow rates [10]. Using this cell type, the group of Bruins et al. systematically investigated the differences and similarities of electrochemical and cytochrome P450 catalysed reactions on different classes of compounds [13]. The list of typical metabolic reactions readily simulated by EC includes oxidative *N*-dealkylation, hydroxylation of activated aromatics and dehydrogenation. As an alternative electrochemical cell type, wall-jet cells have been implemented in the EC-LC-MS set-up used for this study. Requiring low flow rates for sufficient conversion, these cell types have to be used in combination with a switching valve and sample loop, in which the oxidation products are collected before being flushed onto the LC column. In contrast to flow-through cells, the glassy carbon working electrode material of the wall-jet cell can be easily dismantled and exchanged by other working electrode materials, such as gold, platinum or boron doped diamond.

As can be seen from the literature mentioned above [9–13], in recent years, significant progress was made to evaluate the capability of electrochemistry regarding the prediction of metabolic pathways. In this study, the electrochemical simulation of the metabolic pathway of tetrazepam was mimicked and was not only compared to *in vitro* liver cell incubation, but also to *in vivo* studies with healthy patients.

Tetrazepam (Fig. 1) is a well-known therapeutic agent, belonging to the group of 1,4-benzodiazepines. Currently, pharmaceutical specialties containing tetrazepam are Myolastan (Sanofi-Synthelabo, Vienna, Austria) and Epsipam (Will-Pharma, Wavre, Belgium). These pharmaceuticals are frequently prescribed in the treatment of muscle spasm of different origins, like whiplash injury, muscular rheumatism, or slipped spinal disks. In contrast to other benzodiazepines like diazepam (Fig. 1), tetrazepam shows a desirable benefit-risk ratio, since already low amounts of tetrazepam are sufficient to induce the intended anxiolytic and muscle relaxant effects without causing undesirable side effects like sedation and ataxia [14–16].

According to the manufacturer, the metabolism of tetrazepam basically comprises the *N*-demethylation to nortetrazepam and the formation of 3-hydroxytetrazepam, which subsequently undergoes a phase II conjugation reaction with glucuronic acid. Besides that, hydroxytetrazepam, hydroxylated nortetrazepam and some isomeric derivatives were suggested as metabolites [17]. In 2007, Pavlic et al. published a study, strongly indicating the metabolic conversion of tetrazepam to diazepam [18]. By means of gas chromatography with electron-capture detection (GC-ECD) and by GC-MS, Pavlic et al. identified tetrazepam as well as diazepam in urine samples from patients at least 72 h after the intake of one tablet Myolastan. The degradation of tetrazepam to diazepam is of particular interest, since diazepam, also known as the active ingredient in Valium, predominantly acts on the central nervous system, with its primary pharmaceutical effect being sedation. Diazepam has been reported to be abused as illegal drug, especially as date-rape drug in sexual offences. Thus, the presence of

diazepam, deriving from tetrazepam can result in false accusations, when testing on illegal drugs.

The suggested metabolic transformation of tetrazepam to diazepam was further proven by Laloup et al. [19] and by Schubert et al. [20]. Using LC-MS, Schubert et al. identified a number of isomeric hydroxylated, *N*-demethylated and dehydrogenated metabolites. Furthermore, by means of LC-MS/MS, they determined the cyclohexenyl moiety of tetrazepam as the main side of metabolic transformation.

The electrochemical generation of the tetrazepam metabolites, especially the hydroxylation of the cyclohexenyl moiety, is a challenging task, since alkane and alkene hydroxylation have not been reported in electrochemical metabolism studies up to now [13]. To overcome this problem, a wall-jet cell with variable electrode materials and a feasible potential range up to 2 V was implemented in the EC-LC-MS set-up used in this study.

2. Experimental

2.1. Chemicals

Myolastan, containing 50 mg tetrazepam per tablet, was obtained from Sanofi-Synthelabo, Vienna, Austria. Acetonitrile (ACN), methanol, dichloromethane, isopropanol and ammonia solution (25%) were delivered by Merck (Darmstadt, Germany). Potassium dihydrogenphosphate, dipotassium hydrogenphosphate, ammonium acetate, acetic acid and formic acid were obtained from Fluka Chemie (Buchs, Switzerland). Ammonium formate, magnesium chloride hexahydrate and β -glucuronidase from *Helix pomatia*, Type H1 were purchased from Sigma-Aldrich Chemie (Steinheim, Germany). NADPH was ordered from AppliChem (Darmstadt, Germany). Pooled male RLMs (Sprague-Dawley) with a protein concentration of 20 mg/ml and a total P450 enzyme activity of 520 pmol/mg (determined by the method of Omura and Sato [21]) were delivered by BD Bioscience (Woburn, MA, USA).

Purified water for HPLC analysis and sample dilution was generated by a Milli-Q Gradient A 10 system and filtered through a 0.22- μ m Millipak 40 filter unit (Millipore, Billerica, MA, USA). All chemicals were used in the highest quality available.

2.2. Analysis of urine samples

After the intake of one tablet Myolastan (50 mg tetrazepam) by a healthy volunteer, urine samples were collected at different time intervals (1.5; 2.75; 3.75; 4.75; 6.3; 8 and 17.5 h after intake) and prepared for LC-MS analysis. From each collection, 5 ml of the urine sample were cleaned up by solid-phase extraction (SPE). The extraction column (SPE-ED Scan ABN, Applied Separations, Allentown, PA, USA) was conditioned with 2 ml methanol and 2 ml 0.1 M phosphate buffer (pH 6.0). Each urine sample was diluted with 3 ml of distilled water, vortexed and centrifuged (5 min, 4500 rpm). The supernatant was rinsed through the column. Next, the column was washed with 3 ml distilled water, 1 ml 1 M acetic acid, and an aqueous methanol solution (1:10; v/v), centrifuged for 5 min (4500 rpm), and dried with a nitrogen stream to remove any possible remaining aqueous washing solvent. Elution was performed with 2 ml of a solvent mixture of dichloromethane, isopropanol and ammonia (80:20:0.8; v/v/v). The eluate was evaporated to dryness at 60 °C under a nitrogen stream.

For the LC-MS analysis, the dried residue of the clean-up procedure from each sample was redissolved in 250 μ l water with 5% ACN and 0.05% formic acid and directly injected into the LC-MS system.

For the urine sample collected 4 h after Myolastan intake, an enzymatic cleavage of glucuronic acid adducts was performed after the LC-MS analysis. In order to remove the organic solvent

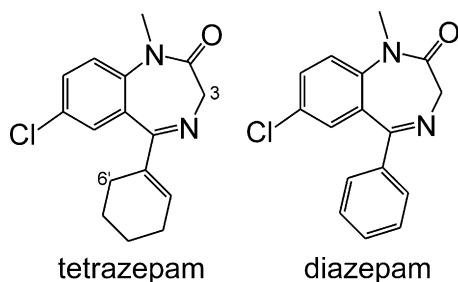


Fig. 1. Structures of tetrazepam and diazepam.

before adding the enzymes, the sample was evaporated to a volume of 50 μl by a slow nitrogen steam. A solution of 4.9 mg β -glucuronidase from *Helix pomatia* (Typ H1) was dissolved in 150 μl 0.1 M ammonium acetate buffer, adjusted to pH 4.9 and was added to the mixture. After incubation at 37 °C for 24 h, proteins were precipitated by adding 350 μl ACN. The mixture was centrifuged and the supernatant was analysed by LC–MS.

2.3. Microsomal incubation

A mixture of microsomal protein and tetrazepam, dissolved in 50 mM phosphate buffer solution and adjusted to pH 7.4, was preincubated for 5 min at 37 °C. Magnesium chloride and NADPH were added to the incubation mixture, which was then further incubated at 37 °C for 90 min. The total volume of the incubation mixture was 500 μl and the final concentrations were as follows: 1.3 mg/ml microsomal protein, 50 μM tetrazepam, 0.5 mM magnesium chloride, 1.2 mM NADPH. Subsequent to the incubation, proteins were precipitated by adding 500 μl ACN. After centrifugation, the supernatant was analysed by LC–MS. As negative control, a second incubation without NADPH was performed.

2.4. Electrochemical simulation

The electrochemical simulation of the oxidative phase I metabolism was performed in an electrochemical wall-jet cell (Flex Cell, Antec Leyden, Zoeterwoude, The Netherlands). Potentials were applied using either the electrochemical detector system Decade II (Antec Leyden) or a homemade potentiostat.

For optimization experiments of the electrochemical conditions, the cell was coupled directly to an electrospray mass spectrometer (micrOTOF, Bruker Daltonics, Bremen, Germany). At a flow rate of 10 $\mu\text{l}/\text{min}$, a 10- μM solution of tetrazepam was passed through the cell by a syringe pump model 74900 (Cole Parmer, Vernon Hills, IL, USA) and a potential range from 0 to 2000 mV was scanned at a scan rate of 5 mV/s. The tetrazepam solution was prepared by dissolving one tablet Myolastan in 10 ml methanol. The insoluble residue of the tablet was removed by filtration and the solution was further diluted to a final concentration of 10 μM tetrazepam. The potential scan was performed testing different solvents for the tetrazepam solution: 20 mM ammonium formate (pH 6.8), 10 mM formic acid (pH 3.1), and 20 mM ammonia (pH 10). In addition, the scan was performed using the different working electrode materials glassy carbon, gold and platinum.

After optimization of the electrochemical conditions, the cell was implemented into an online EC–LC–MS system, in which the electrochemically generated metabolites are subsequently separated on an LC column and detected by MS. The set-up is shown in Fig. 2.

For the electrochemical conversion, a 100- μM solution of tetrazepam in a 10-mM formic acid solution was used. The drug

solution was passed through the electrochemical cell at a flow rate of 10 $\mu\text{l}/\text{min}$. The cell was equipped with a platinum working electrode and was operated at a constant potential of 2000 mV vs. Pd/H₂. The oxidation products, eluting from the EC were collected in a 10-port valve, equipped with a 10- μl injection loop. After filling of the loop, the loop content was flushed onto the LC column by switching the valve and detected by MS.

2.5. LC–MS instruments

LC–MS measurements were performed on two different systems. For fragmentation experiments and measurements in selected ion monitoring (SIM) mode, an HPLC system from Shimadzu (Duisburg, Germany) coupled to a QTRAP mass spectrometer with an electrospray ionization (ESI) source (Applied Biosystems, Darmstadt, Germany) was used. The HPLC system consists of two HPLC pumps (LC-10ADVP), a degasser (DGU-14A), an autosampler (SIL-HTA), a column oven (CTO-10AVP) and an UV detector (SPD-10AVVP) operating at 254 nm. Control of the HPLC–MS system and data handling was carried out by the software Analyst 1.4.1 (Applied Biosystems).

For the determination of exact masses, an HPLC system from Antec Leyden (Zoeterwoude, The Netherlands) coupled to a micrOTOF mass spectrometer, which was equipped with an ESI source (Bruker Daltonics), was used. The components of the HPLC system are two LC 100 pumps, an OR 110 organiser rack with a degasser and a pulse dampener, an AS 100 autosampler and a Decade II column oven. For controlling the HPLC system, the ALEXYS data system (Antec Leyden) was used and for controlling of the micrOTOF and data handling, the software micrOTOFControl 1.1 and DataAnalysis 3.3 was used.

2.6. LC separation conditions

The HPLC separation was performed on a Nucleodur Sphinx RP column (Macherey–Nagel, Düren, Germany) with the dimension 150 mm \times 3 mm, particle size 5 μm and pore size of 100 Å. A flow rate of 400 $\mu\text{l}/\text{min}$ was used. The mobile phase consists of 100 mM aqueous ammonium formate buffer with 0.02% formic acid as eluent A and methanol as eluent B. For the separation, the gradient programme shown in Table 1 was used. The injection volume was 10 μl . The column oven was kept at a constant temperature of 40 °C.

2.7. Mass spectrometric conditions

The analytes were detected in the positive ion mode. The optimized MS conditions, used for the measurements with the QTRAP and the micrOTOF, are listed in Tables 2 and 3.

3. Results and discussion

In this study, different approaches for the investigation of tetrazepam metabolism were performed, including a conventional microsomal approach and a purely instrumental electrochemical simulation. In the following, the results are presented and in particular discussed towards their correlation with metabolism studies based on the analysis of urine samples from patients after tetrazepam intake.

Table 1

Gradient profile used for the separation of tetrazepam and its metabolites.

Time (min)	0	2	18	20	21	26
Methanol (%)	60	60	90	90	60	60

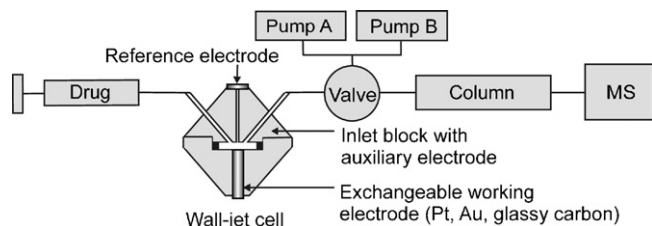


Fig. 2. Online EC–LC–MS set-up for the electrochemical generation of oxidative metabolites with subsequent LC separation and detection by mass spectrometry. A 10-port valve equipped with a 10- μl injection loop allows the use of low flow rates (10 $\mu\text{l}/\text{min}$) for the electrochemical conversion in combination with high flow rates for the LC separation (400 $\mu\text{l}/\text{min}$).

Table 2

QTRAP parameters used for the detection of tetrazepam and its metabolites in selected ion monitoring mode and in enhanced product ion mode for fragmentation experiments.

Parameter	EC-LC-QTRAP SIM mode/fragmentation
Declustering potential (V)	30/35
Entrance potential (V)	6/12
Curtain gas (N ₂) (psi)	25
Ion spray voltage (V)	5500
Temperature (°C)	400
Nebulizer (N ₂) (psi)	50
Dry gas (N ₂) (psi)	50
Cell entrance potential (V)	-12
Collision energy (V)	-25
Cell exit potential (V)	-10

Table 3

MicroTOF parameters used for the detection of tetrazepam and its metabolites during optimization of the electrochemical cell (EC-TOF) and for the determination of exact masses in EC-LC-MS measurements.

Parameter	EC-TOF/EC-LC-TOF <i>m/z</i> 200–600
End plate offset (V)	-500
Capillary (V)	-3750
Nebulizer gas (N ₂) (bar)	0.8/1.3
Dry gas (N ₂) (bar)	3.5/4.5
Dry temperature (°C)	200
Capillary exit (V)	116.7
Skimmer 1 (V)	39
Skimmer 2 (V)	22.4
Hexapole 1 (V)	24
Hexapole 2 (V)	20.6
Hexapole RF (V)	90
Transfer time (μs)	49
Prepulse storage (μs)	1
Detector (V)	-1300

3.1. Analysis of urine samples

Urine samples at 1, 2, 4, 6, 8 and 17 h after Myolastan intake were analysed by LC-MS. The main excretion of tetrazepam metabolites was found between 4 and 6 h and no additional metabolites were found in samples collected later or earlier. Therefore, the chromatogram of the 6 h sample was studied in detail and was further used for comparison with the microsomal approach and the electrochemical simulation.

As shown in Fig. 3 and Table 4, all detected metabolites in the chromatogram of the 6-h urine sample elute earlier from the reversed-phase column than the non-metabolised tetrazepam. Five different isomers of hydroxylated tetrazepam (tetrazepam + O) were found in the urine samples (peaks 2, 3, 6, 8, 10). According to previous tetrazepam studies [20], the most likely hydroxylation site

Table 4

Molecular formula of tetrazepam metabolites, determined by LC-TOF/MS. The deviation of measured *m/z* to the theoretical *m/z*, given as relative mass deviation (ppm) = $((m/z_{\text{experimental}} - m/z_{\text{calculated}}) / m/z_{\text{calculated}}) \times 10^6$, was for all metabolites below 5 ppm. For peak identification, refer to Fig. 3.

Peak	<i>m/z</i>	Molecular formula	Transformation of tetrazepam	Urine	RLMs	EC
1	291	C ₁₅ H ₁₆ ClN ₂ O ₂	-CH ₃ + O	x	x	
2	305	C ₁₆ H ₁₈ ClN ₂ O ₂	+O	x	x	x
3	305	C ₁₆ H ₁₈ ClN ₂ O ₂	+O	x	x	x
4	303	C ₁₆ H ₁₆ ClN ₂ O ₂	-H ₂ + O	x	x	
5	301	C ₁₆ H ₁₄ ClN ₂ O ₂	-2H ₂ + O	x		x
6	305	C ₁₆ H ₁₈ ClN ₂ O ₂	+O	x		x
7	305	C ₁₆ H ₁₈ ClN ₂ O ₂	+O		x	x
8	305	C ₁₆ H ₁₈ ClN ₂ O ₂	+O	x	x	x
9	285	C ₁₆ H ₁₄ ClN ₂ O	-2H ₂	x	x	x
10	305	C ₁₆ H ₁₈ ClN ₂ O ₂	+O	x	x	x
11	275	C ₁₅ H ₁₆ ClN ₂ O	-CH ₃	x	x	x
12	287	C ₁₆ H ₁₆ ClN ₂ O	-H ₂	x	x	x

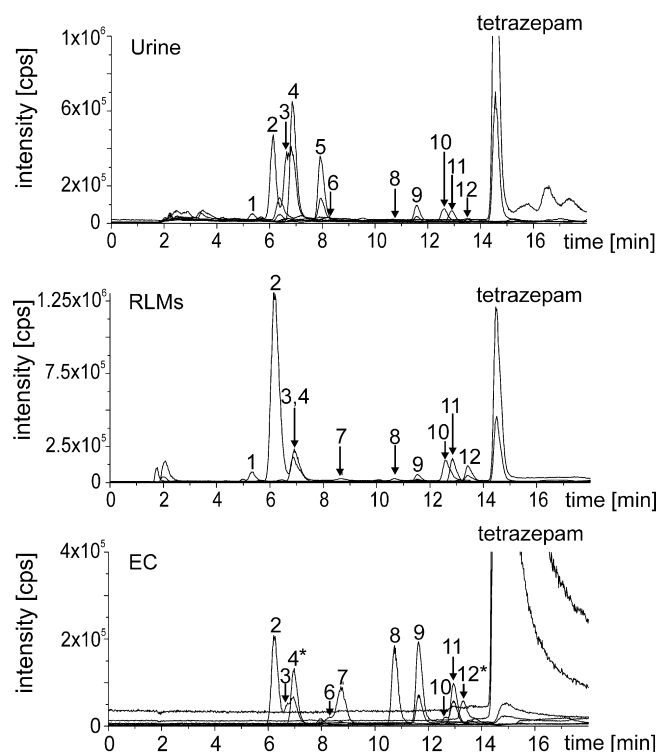


Fig. 3. Comparison of the oxidative metabolites of tetrazepam found in urine (6 h after Myolastan intake), in an incubation mixture with rat liver microsomes (RLMs) and in an electrochemical simulation (EC). Peak assignment: 1, tetrazepam-CH₃ + O; 2, 3, 6–8, 10, tetrazepam + O; 4, tetrazepam-H₂ + O; 5, tetrazepam-2H₂ + O; 9, tetrazepam-2H₂; 11, tetrazepam-CH₃; 12, tetrazepam-H₂; *Peaks which were also present in a Myolastan solution without electrochemical oxidation.

in the tetrazepam molecule is the cyclohexenyl group and not to the common doctrine the hydroxylation to 3-hydroxytetrazepam. For further confirmation of the hydroxylation site, the fragmentation pattern was studied. Tetrazepam derivatives with a hydroxy group at the position 3 may be distinguished from tetrazepam and its other metabolites by their fragmentation pattern. In contrast to tetrazepam, the fragmentation of 3-hydroxytetrazepam does not result in a fragment ion correlating to the loss of CO, but only in fragment ions correlating to the loss of H₂O and H₂O plus CO (Fig. 4) [20]. For the intense peaks 2, 3 and 10 in the extracted ion chromatogram *m/z* 305 (Fig. 3), fragmentation experiments show a significant loss of CO (see Fig. 5a for peak 2). For the less abundant isomers, the signal intensity was not sufficient to obtain a significant fragment ion corresponding to a loss of CO. Thus, it cannot be excluded that one of these isomers is 3-hydroxytetrazepam.

The insertion of an oxygen atom in the cyclohexenyl group may take place under the formation of a hydroxy group or by an epoxidation of the double bond. The epoxide may rearrange under the formation of a ketone, which is expected to be less polar than the hydroxy metabolites and thus will be the last eluting isomer. Assuming that the position 1' (Fig. 1) is sterically hindered, the number of possible isomeric compounds fits to the number of detected tetrazepam + O metabolites.

Besides the hydroxylated metabolites, dehydrogenated metabolites (tetrazepam-H₂, peak 12 and tetrazepam-2H₂, peak 9) are detected. The abstraction of four hydrogen atoms in the cyclohexenyl group of the tetrazepam molecule results in the formation of an aromatic ring and is therefore thermodynamically favoured. In addition, for the compound tetrazepam-H₂, product ion mass spectra confirm the dehydrogenation in the cyclohexenyl group, since fragment ions corresponding to the loss of CO were found. The dehydrogenation product tetrazepam-2H₂ is further known as diazepam

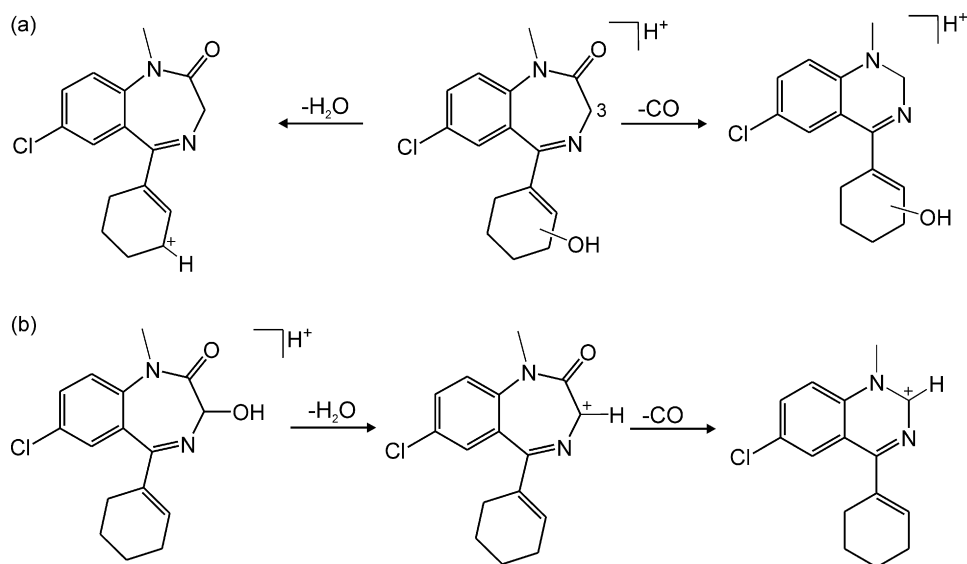


Fig. 4. Structure of significant MS/MS fragments of a tetrazepam species hydroxylated at the cyclohexenyl moiety and of 3-hydroxytetrazepam. The loss of CO indicates a hydroxylation at the aromatic cyclohexenyl group, whereas the loss of H₂O in a fragment ion corresponding to the loss of CO indicates the presence of 3-hydroxytetrazepam.

and is of particular interest, since diazepam effects on the organism include sedation and ataxia and the presence of diazepam may lead to positive results when testing on illegal drugs.

Furthermore, hydroxylated products of these dehydrogenated products were detected (tetrazepam-H₂+O, peak 4 and tetrazepam-2H₂+O, peak 5). Again, the product ion spectra of both metabolites indicate a dehydrogenation and an insertion of oxygen in the cyclohexenyl ring by the presence of a fragment ion corresponding to the loss of CO. The loss of two hydrogen atoms in combination with the insertion of oxygen may result from the formation of a double bond in combination with a hydroxyl group, a double bond formation with subsequent epoxidation or from the formation of a ketone. Compared to the elution order of the dehydrogenated species, the elution order of the hydroxylated dehydrogenated species is inverted. Tetrazepam-2H₂+O appears to be less polar than tetrazepam-H₂+O. This fact might indicate that tetrazepam-2H₂+O is a ketone or epoxide, whereas tetrazepam-H₂+O is a hydroxylated species.

Another typical metabolic reaction, the N-dealkylation of an amide, also becomes apparent when analysing the urine sample. The N-demethylation of tetrazepam results in the formation of nortetrazepam, which elutes from the column shortly before

tetrazepam itself. In addition, a hydroxylated nortetrazepam species was found, but due to very low signal intensity, no further structure information about the position of the oxygen atom was obtained by its fragmentation.

The information gained by the analysis of the urine sample is summarised in the reaction scheme shown in Fig. 6 and in Table 4. For each detected metabolite, one possible structure is presented and the suggested degradation pathway of tetrazepam to diazepam, as previously published by Schubert et al. [20] is shown. All metabolites detected in the analysis of the urine sample are in good accordance with the metabolites detected in earlier studies, as well as with the suggested metabolic pathway. Schubert et al. reported two further minor metabolites, including the doubly hydroxylated tetrazepam+2O and tetrazepam+2O-H₂. In our study, these two metabolites could not be detected at a significant signal to noise ratio.

3.2. Microsomal approach

In order to examine the metabolic pathway of drug compounds, the incubation with rat liver microsomes is a conventional, well-known method. Therefore, this method was performed on

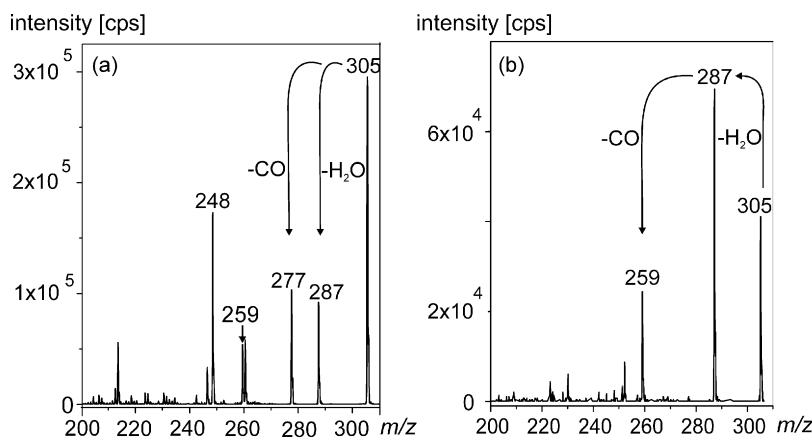


Fig. 5. (a) Fragmentation pattern of the metabolite tetrazepam + O (*m/z* 305, peak 2), appearing in the urine sample and in the electrochemical simulation and (b) fragmentation pattern of the metabolite tetrazepam + O (*m/z* 305, peak 7), appearing only in the electrochemical simulation.

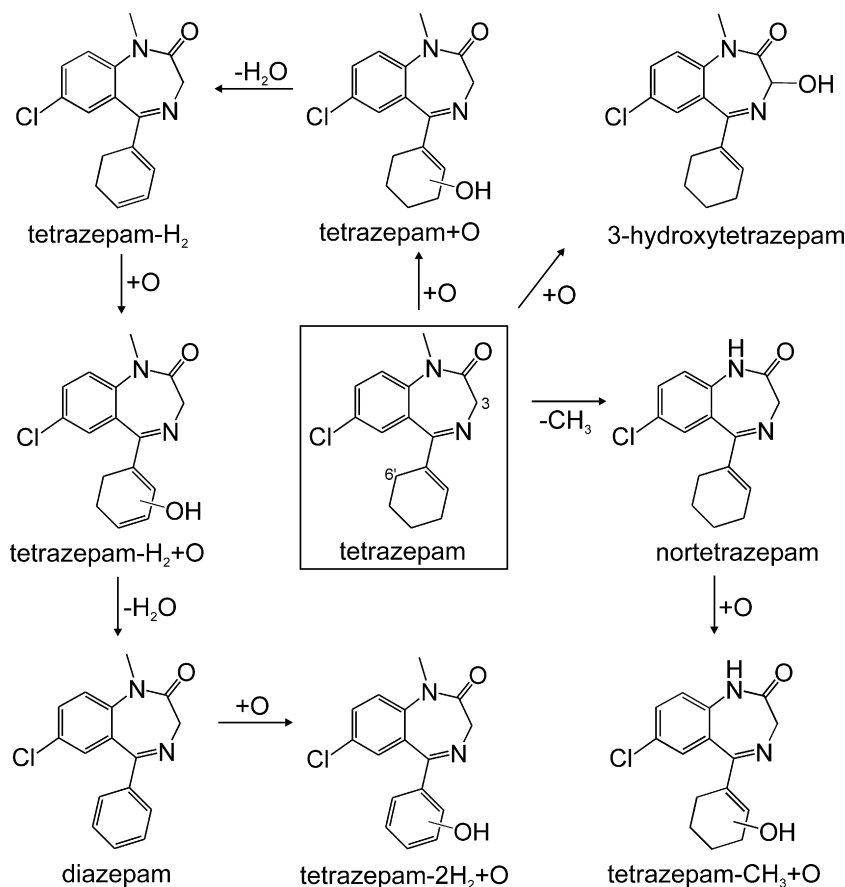


Fig. 6. Oxidative metabolites of tetrazepam and the suggested degradation pathway of tetrazepam to diazepam. All metabolites included in this pathway were simulated by electrochemistry.

tetrazepam and the results were compared to the metabolites detected in the urine sample and to the purely instrumental electrochemical method. The comparison of the chromatograms is shown in Fig. 3. Compared to the urine sample, only two metabolites, being tetrazepam+O-2H₂ (peak 5) and one isomer of tetrazepam+O (peak 6), were not found after the microsomal incubation. The expression of the different isoforms of P450 with its different catalytic activities towards metabolic reactions varies in each organism. Thus, the metabolism in humans and in rat liver microsomes may result in different metabolites or a different quantitative distribution of the metabolites. This explains the two missing metabolites in the microsomal approach.

For the additional tetrazepam+O metabolite (peak 7), detected in the LC-MS analysis of the microsomal approach, it was suggested that it is 3-hydroxytetrazepam. As mentioned, the degradation pathway of tetrazepam postulated by the manufacturer includes the formation of 3-hydroxytetrazepam followed by a conjugation reaction with glucuronic acid. Since no activated glucuronic acid was added to the incubation mixture, an additional 3-hydroxytetrazepam peak compared to the urine sample was expected in the chromatogram. Due to the low signal intensity, the fragmentation pattern of the metabolite did not yield further information about the position of the oxygen insertion. A second approach to identify the metabolite was the hydrolysis of the glucuronic acid adduct in the urine sample by β -glucuronidase. After a 24-h incubation of the urine sample with β -glucuronidase, the glucuronic acid adduct with m/z 481 did no longer appear in the chromatogram, but due to the low amount of the precursor adduct itself, no additional hydroxytetrazepam peak could be detected. The absence of 3-hydroxytetrazepam after the hydrolysis of the glu-

cronic acid adduct supports the previously published results by Schubert et al. [20], who showed that the cyclohexenyl moiety and not the position 3 is the main hydroxylation site in the molecule.

3.3. Electrochemical simulation

3.3.1. Optimization of the electrochemical conditions

The best conversion of tetrazepam into its expected metabolites was achieved using the 10 mM formic acid solution and platinum as working electrode material operating at a potential of 2 V. Due to the unconventionally high oxidation potential, it cannot be excluded that partial electrolysis of the aqueous solvent takes place. The working electrode was cleaned between each oxidation step by flushing with a solution of 50% ACN in water. When dismantling the working electrode after an oxidation, no adsorption residue was visible.

3.3.2. Online EC-LC-MS experiments

The chromatogram of the oxidation products of tetrazepam is shown in Fig. 3. Compared to the urine sample, two metabolites were missing, the hydroxylated nortetrazepam (tetrazepam-CH₃+O, peak 1) and the metabolite tetrazepam-2H₂+O (peak 5), which was also absent in the microsomal incubation. Besides these two, all other metabolites were electrochemically generated, including dehydrogenation products, demethylation products and hydroxylation products. As shown for the urine sample, five of the tetrazepam+O isomers bear an additional oxygen atom in the cyclohexenyl moiety. In the literature, discussing the oxidative simulation of phase I metabolism, the hydroxylation of alkanes has not been reported yet. However, using an unconventionally high

potential of 2 V, we were able to simulate the insertion of oxygen at five different positions in the cyclohexenyl ring of tetrazepam, thus including alkyl and allyl positions as well as an oxidation directly at the double bond.

As already described for the microsomal approach, the additional tetrazepam + O metabolite (peak 7, Fig. 3) was suggested to be 3-hydroxytetrazepam. In contrast to the microsomal approach, the signal intensity was sufficient for further fragmentation studies after using electrochemistry. By an absence of a fragment ion corresponding to the loss of CO, the pattern strongly indicates the formation of 3-hydroxytetrazepam (Fig. 5b). Further possible hydroxylation sites in the molecule are the cyclohexenyl moiety, the aromatic ring or the formation of an N-oxide. However, all of these oxidation products should result in a fragment ion corresponding to the loss of CO in MS/MS experiments, which was not observed.

The hydroxylation of nortetrazepam is a reaction, which is as likely to happen as the hydroxylation of tetrazepam itself. Hence, the absence of tetrazepam-CH₃ + O might simply result from a very low amount of electrochemically generated demethylated tetrazepam. Due to the stability of the initial radical cation in the oxidation mechanism, the oxidation potential for tertiary alkyl amines increases with decreasing chain length [13]. Thus, a demethylation is generally not a favoured electrochemical reaction. In this case, it is likely that the electron withdrawing effect of the neighbouring carbonyl group further influences the oxidation reaction.

The absence of tetrazepam-2H₂ + O can be also explained by the low amount of produced diazepam itself. In addition, the oxidation of a non-activated aromatic ring has not been simulated in electrochemical metabolism studies up to now and was thus not expected in this experiment.

4. Conclusion

In this study, a purely instrumental method, based on an electrochemical oxidation in combination with an online HPLC separation and mass spectrometric detection was used to examine the metabolic pathway of tetrazepam. The comparison with the analysis of urine sample from patients after tetrazepam intake clearly demonstrates that the entire metabolic degradation of tetrazepam to diazepam can be predicted by electrochemical simulation. The implementation of a wall-jet cell with exchangeable electrode materials proved to be a valuable tool in the EC-LC-MS set-up. Up to now, one limitation of the electrochemical method was the impossibility to mimic the metabolic hydroxylation of alkanes and alkenes [13]. In the present study, this problem was overcome by using a platinum working electrode in combination with an enhanced potential range up to 2000 mV. Thus, the hydroxylation of the tetrazepam cyclohexenyl group at five different positions was successfully performed.

In order to judge the feasibility of the electrochemical method as a tool in the prediction of metabolites in drug development studies,

it was further compared to a conventional microsomal approach. Both methods were able to predict almost all metabolites found in the urine sample. In the microsomal approach, two metabolites were missing, which probably results from the different expression of P450 isoforms in each organism. In the electrochemical approach, two metabolites were missing as well. Since both metabolites are products of subsequent oxidation reactions, which are in principle electrochemically accessible, it is suggested that the concentration of oxidative intermediate is too low for the detection of the final product. For one metabolite, significantly higher signal intensity is achieved in the electrochemical study compared to the *in vivo* and *in vitro* approaches. Thereby, an advanced structure elucidation by the fragmentation pattern could be performed. In conclusion, the comparison of both methods points out that electrochemistry combined with LC/MS is a promising supplementary tool to the conventional *in vitro* methods in the prediction of metabolic processes.

Acknowledgements

This work was supported by grants from the Deutsche Forschungsgemeinschaft (Bonn, Germany) and the Fonds der Chemischen Industrie (Frankfurt am Main, Germany). Furthermore, financial support by the Austrian Research Promotion Agency (FFG, Österreichisches Sicherheitsforschungs – Förderprogramm KIRAS – eine Initiative des Bundesministeriums für Verkehr, Innovation, Technologie (BMVIT), Projekt 813786) is acknowledged.

References

- [1] E.F.A. Brandon, C.D. Raap, I. Meijerman, J.H. Beijnen, J.H.M. Schellens, *Toxicol. Appl. Pharmacol.* 189 (2003) 233.
- [2] F.P. Guengerich, E.M. Isin, *Acta. Chim. Solv.* 55 (2008) 7.
- [3] G. Hambitzer, J. Heitbaum, *Anal. Chem.* 58 (1986) 1067.
- [4] K.J. Volk, M.S. Lee, R.A. Yost, A. Brajter-Toth, *Anal. Chem.* 60 (1988) 720.
- [5] K.J. Volk, R.A. Yost, A. Brajter-Toth, *J. Chromatogr.* 474 (1989) 231.
- [6] K.J. Volk, R.A. Yost, A. Brajter-Toth, *Anal. Chem.* 61 (1989) 1709.
- [7] K.J. Volk, R.A. Yost, A. Brajter-Toth, *J. Electrochem. Soc.* 137 (1990) 1764.
- [8] T.A. Getek, W.A. Korfmacher, T.A. McRae, J.A. Hinson, *J. Chromatogr.* 474 (1989) 245.
- [9] S.M. Van Leeuwen, B. Blankert, J.-M. Kauffmann, U. Karst, *Anal. Bioanal. Chem.* 382 (2005) 742.
- [10] W. Lohmann, U. Karst, *Anal. Bioanal. Chem.* 391 (2008) 79.
- [11] W. Lohmann, U. Karst, *Anal. Bioanal. Chem.* 386 (2006) 1701.
- [12] W. Lohmann, U. Karst, *Anal. Chem.* 79 (2007) 6839.
- [13] U. Jurva, H.V. Wikström, A.P. Bruins, *Rapid Commun. Mass Spectrom.* 14 (2000) 529.
- [14] P.E. Keane, A. Bachy, M. Morre, K. Biziere, *J. Pharmacol. Exp. Ther.* 245 (1988) 699.
- [15] P.E. Keane, J. Simiand, M. Morre, K. Biziere, *J. Pharmacol. Exp. Ther.* 245 (1988) 692.
- [16] M. Pellkofer, M. Paulig, *Med. Klin. (Munich)* 84 (1989) 5.
- [17] H. Maurer, K. Pfleger, *J. Chromatogr.* 422 (1987) 85.
- [18] M. Pavlic, K. Libiseller, P. Grubwieser, H. Schubert, W. Rabl, *Int. J. Legal Med.* 121 (2007) 169.
- [19] M. Laloup, M. del Mar Ramirez Fernandez, M. Wood, V. Maes, G. De Boeck, Y. Vanbeckevoort, N. Samyn, *Anal. Bioanal. Chem.* 388 (2007) 1545.
- [20] B. Schubert, M. Pavlic, K. Libiseller, H. Oberacher, *Anal. Bioanal. Chem.* 392 (2008) 1299.
- [21] T. Omura, R.J. Sato, *J. Biol. Chem.* 239 (1964) 2370.